Available online at www.sciencedirect.com
SCIENCE DIRECT
Polymer 46 (2005) 1095–1104
polymer
www.elsevier.com/locate/polymer

Atom transfer radical polymerization from silica nanoparticles using the 'grafting from' method and structural study via small-angle neutron scattering

A. El Harrak, G. Carrot*, J. Oberdisse, J. Jestin, F. Boué

Laboratoire Léon Brillouin, CEA/CNRS, Bâtiment 563, CEA/Saclay, 91191 Gif-sur-Yvette, France

Accepted 30 September 2004
Available online 21 December 2004

Abstract

Polymer chains were grafted from silica beads (colloidal sol in dimethylacetamide) by atom transfer radical polymerization (ATRP), via the 'grafting from' method. The grafting of the initiator onto the silica surface was done in two steps. First, thiol-functionalization of the surface was achieved via silanization with a mercaptopropyl triethoxysilane. Second, we performed an over-grafting of the surface by reacting the thiol with 2-bromoisobutyryl bromide to generate the halogen-functional ATRP initiator. The nanoparticles were kept in solution (in the same solvent) at each stage of the functionalization (even during the purification steps), as this is the only way to avoid irreversible aggregation. Then, the polymerization of styrene was conducted. Control of both the molecular weight and the density of grafted chains can be achieved by this method. Careful characterization such as gel permeation chromatography, ^{29}Si CP/MAS NMR, elemental analysis, infrared spectroscopy and thermo-gravimetric analysis is performed. The state of dispersion of the grafted nanoparticles is followed in details by small angle neutron scattering and results obtained from this technique are presented here as well as the way the SANS data can be treated. Connection is systematically done between the information provided by this technique and the improvement of the synthetic procedure.

Keywords: Organic–inorganic silica nanoparticles; Grafting from; Colloidal stability

1. Introduction

Grafting polymers onto nanoparticles in order to elaborate organic/inorganic nanocomposites has led to an increasing interest in the last decade [1–3]. One possible interest is the better handling of the unusual properties of the nanoparticles (optical, electronic, catalytic) due to the control of interparticle distance by the polymer grafted onto it. In the present work, we focused on the improvement of the mechanical properties given by the inclusion of nano-fillers (silica nanoparticles) in the polymer matrix [4–6]. Here the grafting of polymer chains onto the particle will serve to improve the compatibility between the particles (silica surface is hydrophilic) and the polymer matrix (generally hydrophobic). Two general routes has been used to graft linear polymer chains at the surface of the particles. One method is grafting functionalized polymers onto particles [7]. This technique, namely the 'grafting onto' method, has the disadvantage of low degrees of grafting because of steric hinderance. Another method called the 'grafting from' method, consists in grafting first an initiator molecule in order to perform the polymerization from the particle surface [8,9]. This method combined with the use of controlled polymerisations such as atom transfer radical polymerization (ATRP) has shown to give very satisfactory results in terms of degree of grafting and control in the polymerization processes. It has been widely studied for planar surfaces [10–19] and few works on spherical particles have also been reported [20–29].

In our work, grafting of the initiator has been done in two steps: the functionalization of the surface with a mercapto-silane followed by an over-grafting from the thiol group to generate the bromine function (initiating specie in the ATRP process). A similar technique has been used for the

* Corresponding author. Tel.: +33 1 69 08 60 37; fax: +33 1 69 08 82 61.
E-mail address: carrot@llb.saclay.cea.fr (G. Carrot).

0032-3861/$ - see front matter © 2004 Elsevier Ltd. All rights reserved.
doi:10.1016/j.polymer.2004.11.046

functionalization of silica wafers and was found to give better results in terms of control and degree of grafting compare to the 'one step' grafting [15].

We performed the functionalization onto colloidal silica nanoparticles ($\approx$10 nm in diameter) dispersed in dimethylacetamide. One feature of the work is that for each reaction step, we kept the nanoparticles in the same solvent to avoid aggregation that may occur by drying the particles or changing the solvent conditions. Small angle neutron scattering (SANS) was used to check the preservation of the colloidal stability through the different reaction steps. This technique is particularly appropriate for such systems for several reasons: range of scales attainable, and the possibility to see either the silica, or the chains, using index matching. The matching conditions and the SANS data treatments had to be adapted to this particular system.

2. Experimental procedures

2.1. Materials

Styrene was purified by distillation from calcium hydride. Mercaptopropyl triethoxysilane (MPTS) was purchased from ABCR. Anhydrous pyridine (99.8%), dimethylaminopyridine (DMAP), Dimethylacetamide (DMAc), 2-bromoisobutyrate bromide, *N*,*N*,*N*′,*N*′,*N*″-pentamethyldiethylenetriamine (PMDETA), copper (I) bromide (99.999%, stored under nitrogen), were used as received from Aldrich. Silica nanoparticles in a 20 wt% sol in dimethylacetamide, were kindly provided by Nissan (DMAC-ST) and used as received. SANS characterization of dilute solutions can be described by a log-normal distribution with a variance $\sigma = 0.365$ and a mean diameter of 10 nm, hence a specific area of 190 m^2/g.

2.2. Synthesis

2.2.1. Silanization of colloidal silica nanoparticles in dimethylacetamide

The silica dispersion (52.7 g of 20 wt% SiO_2 in dimethylacetamide) was added to a 250 mL round-bottom flask with a magnetic stir bar and fitted with a reflux condenser. Mercaptopropyl triethoxysilane (MPTS) (0.7 mL, 3.15 mmol) was added and the reaction mixture was gently refluxed for a period of 4 h. Maximum grafting was obtained after that time and percentage of silane condensed on the surface of silica nanoparticles was determined from elemental analysis of sulfur.

2.2.2. Over-grafting of 2-bromoisobutyrate bromide onto the thiol-functional silica nanoparticles

DMAP (0.17 g, 1.4 mmol) and DMAc (40 mL) were introduced in a three necks flask under nitrogen. Then, 10 mL of the previously silanized particles dispersion in DMAc was added through a filter (0.45 μm) to obtain a 4 wt% SiO_2 solution. Then, 2-bromoisobutyrate bromide (0.32 g, 1.4 mmol) diluted in 10 mL of DMAc was added dropwise to the reaction mixture. The amount of DMAc added to the final solution mixture was adjusted to dilute the solution to 3.5 wt% of SiO_2. After 48 h, the reaction mixture was filtered under gas pressure using a Millipore Ultrafiltration apparatus with a 30,000 Dalton pores diameter filter (regenerated cellulose) purchased from Millipore. The solution was filtered four times. Each time, 50 mL of the obtained solution were diluted with 300 mL of DMAc and then concentrated to the initial volume.

Surface density of initiator. The number of initiator molecules grafted onto the surface of the nanoparticles is correlated to the number of bromine obtained from elemental analysis according to the following equation:

$$\text{no. of molecules per nm}^2 = \frac{n_{\mathrm{Br}} \times N_{\mathrm{A}}}{A \times 10^{18}} \quad (1)$$

where N_A is the Avogadro number, A is the specific area of the silica particles in nm^2 and n_{Br} is the number of moles of bromine determined from elemental analysis relative to the amount of silicone atoms.

2.2.3. ATRP of styrene from 2-bromo-thioisobutyrate nanosilica colloids (BIB-SiO_2)

A typical example of grafting polymerization is as follows. The sol of silica particles with grafted initiator ($BIBSiO_2$) in DMAc (20 mL of a 3.5%wt SiO_2 sol), was added to a mixture of Cu(I)Br (26 mg, 0.18 mmol), PMDETA (31.5 mg, 0.18 mmol) in a 250 mL three-neck flask under nitrogen. The CuBr/PMDETA/$BIBSiO_2$ molar ratio was generally 0.6:0.6:1 (for styrene). Some free initiator (the same molecule as the one used in the solution polymerization) was also added to the solution (34 mg, 0.15 mmol). All liquids were deoxygenated by bubbling with nitrogen for 30 min. The reaction mixture was stirred until it became homogeneous. Styrene (35 mL, 0.3 mol) was added dropwise within the first hour, in order to avoid gelification which could be induced by the change in the polarity of the solvent mixture. Then, the reaction flask was heated to 110 °C. Kinetic samples were taken via purged syringes and were used to determine conversion by gravimetry. Molar mass evolution was obtained from gel permeation chromatography (GPC), after sample purification through precipitation in methanol. Since non-grafted initiator was added to the reaction mixture, some free chains should be formed. In order to remove them, the final solution could be diluted with THF and centrifugated at 16,000***g***. We removed the supernatant until no more polymer could be detected by infra-red (FT-IR).

2.3. Characterization

2.3.1. Size exclusion chromatography analysis

Number average molecular weights (M_n), weight average molecular weight (M_w), and molecular weight distribution

(M_w/M_n) were determined using gel permeation chromatography (GPC) in THF at 30 °C and a flow rate of 1 mL min^{-1}. Two 7.5 mm diameter × 300 mm Polymer Labs 5 μm particle diameter mixed-D PLgel columns were connected in line to a Shimadzu LC-10AD pump, a degasser (Erma, ERC-3312), a Shimadzu RID-6A differential refractive index (DRI) detector and a PD 2000 (Precision Detectors, Inc.) two-angle light scattering (TALLS) detector. The static measurements were done both at 15 and 90°, and simultaneously coupled to a dynamic light scattering analysis.

2.3.2. NMR, FT-IR analysis and thermal measurement

Solid state ^{29}Si CP/MAS NMR spectra were obtained from an Avance 300 instrument (with a 4 mm probe at the magic angle rotation of 4 Hz). Quantitative experiments were performed from simple impulsion (90° pulse and 120 s. for recycling time). Non quantitative experiments were obtained from cross-linked polarization (contact time: 2 ms). Infra-red spectra were obtained from a FT-IR spectrometer from Nicolet (Avatar 360). Thermo-gravimetric analysis (TGA) was performed on a TA instrument Q50, at a scan rate of 20 °C min^{-1} to 800 °C under air.

2.3.3. SANS measurements

SANS-experiments have been performed on the small-angle PACE spectrometer at Laboratoire Léon Brillouin (CEA/CNRS) at Saclay and on the small-angle V4 spectrometer at BENSC of Hahn-Meitner Institut (HMI) in Berlin. Three configurations were used in Saclay (wavelength $\lambda_0 = 6.0$ Å, $D_{\text{sample-to-detector}} = 1$ and 4.60 m, and $\lambda_0 = 16.8$ Å, $D_{\text{sample-to-detector}} = 4.60$ m), covering a q-range of 0.003–0.26 $Å^{-1}$. Three configurations were also used in Berlin ($\lambda = 6$ Å, $D_{\text{sample-to-detector}} = 1$, 4, and 12 m). In all cases scattered intensities were divided by transmission and sample thickness (1 and 2 mm), corrected from empty cell scattering and normalized to scattering from light water. Absolute units (cm^{-1}) were obtained by measuring the incident flux at LLB-Saclay, and from transmission and incoherent scattering of water at HMI-Berlin, with comparable results. Special care was taken for the analysis and subtraction of the incoherent scattering, namely by measuring scattering from blanks of identical chemical composition. Difficulties in background subtraction due to the complex composition of some samples are discussed in the following.

Interpretation of scattering curves of silica beads with grafted polymer may be rather complex. Due to low scattering, fitting with more elaborate models [30] could not be achieved yet. Our approach was to mask different contribution by choosing the appropriate H/D solvent mixtures. Our simplified discussion of the results is based on three scattering laws. The first one is the scattering from spherical beads, which is a well-known analytical function [31]. Its important limits are the high-q scattering (Porod-domain, $I \propto q^{-4}$) which contains information on the surface structure, and the low-q scattering (Guinier-domain). At high dilution, its expression for monodisperse spheres reads:

$$I(q) = \Phi_{si}\Delta\rho^2 V_b \exp(-q^2R^2/5)$$
$$= \Phi_{si}\Delta\rho^2 V_b \exp(-q^2R_g^2/3) \quad (2)$$

where Φ_{si} denotes the volume fraction (of silica beads in our case), $\Delta\rho$ is the scattering length density contrast with respect to the solvent, and V_b is the volume of a bead of radius R (or of radius of gyration, R_g). From Eq. (2), the general prefactor $I(q \to 0) = \Phi_{si}\Delta\rho^2 V_b$ is seen to be directly proportional to the contrast squared, $\Delta\rho^2$. We take advantage of this in the contrast variation experiment described below. Note that this expression of $I(q \to 0)$ holds also for completely different geometries, like macromolecules. The scattering functions of the latter are easily separated in two regimes. In the Guinier regime (accessible only for small chain size and at high dilution), the intensity starts at $q \to 0$, from the same general prefactor, and its initial decay is also described by an exponential $\exp(-q^2R_g^2/3)$, where R_g is the radius of gyration of the macromolecules. At higher angles, an intermediate regime can be observed for large enough molecules:

$$I(q) \propto 1/q^{Df} \quad (R_g^{-1} < q < a^{-1}) \quad (3)$$

Here D_f denotes the fractal dimension of the polymer, and a the characteristic length scale of a monomer.

Finally, in the case of the scattering from more concentrated colloidal suspensions, the interaction between neighbouring colloids may induce some liquid-like order, leading to a peak at the most probable distance D^* in the bead–bead pair-correlation function. Its Fourier transform gives the interparticle structure factor, peaked at $q_o = 2\pi/D^*$. This peak can be seen in the scattered intensity. If it is well-defined, its position can be used to estimate the average volume of the colloidal objects.

$$V_{ob} = (2\pi/q_o)^3 \Phi_{si} \quad (4)$$

In the case of a slight aggregation of particles, e.g. the average aggregation number $N_{agg} = V_{ob}/V_b$ can be deduced.

Solvent background. The silica beads are suspended in DMAc, a rather uncommon organic solvent, as least for scattering experiments. In order to learn about the background generated by this solvent, we have conducted a series of experiments with varying protonated-to-deuterated DMAc ratio. The intensities are shown in Fig. 1. As expected, the most deuterated solvents have the smallest background. Note that all samples of this series except the completely protonated one have been measured in 2 mm Hellma cells, in order to ensure high enough transmission. Rather surprisingly, the intensity scattered by H/D-mixtures is not completely flat, but decreases slightly with q, whereas the pure H- and D-solvents show no q-dependence. In order to analyse this behaviour, we have split the background into its purely incoherent contribution and the one due to the random mixture of molecules with different coherent

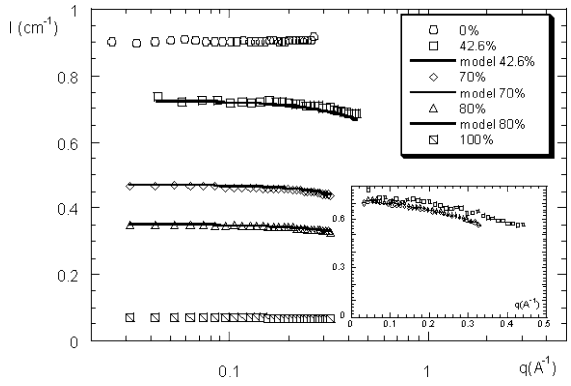

Fig. 1. Intensity scattered from mixtures of deuterated and protonated solvent as a function of wave-vector q. The symbols represent the measured values for each volume fraction of deuterated solvent Φ_D, whereas the continues curves are model results (see text for details). In the inset, the master curve (intensity divided by Φ_D $(1-\Phi_D)$) calculated for all Φ_D is shown.

scattering lengths [32]. The first part can be obtained by a linear interpolation between the completely protonated ($0.9\ cm^{-1}$) and the completely deuterated ($0.069\ cm^{-1}$) solvents, and is indeed completely flat because it is purely incoherent, i.e. it contains no structural information:

$$\frac{d\Sigma}{d\Omega}\Big|_{inc} = \Phi_D\ 0.069\ cm^{-1} + (1-\Phi_D)0.9\ cm^{-1} \quad (5)$$

where Φ_D is the volume fraction of deuterated molecules. The second part is due to the mixture, and can be seen as a form factor of the solvent molecules, or better as the characteristic length scale of contrast heterogeneities:

$$\frac{d\Sigma}{d\Omega}\Big|_{mix} = \Phi_D(1-\Phi_D)(b_{c,H}-b_{c,D})^2\frac{f(q)}{v} \quad (6)$$

where b_c is the coherent scattering length of a solvent molecule, v is its volume calculated from the density and the molecular weight ($v = 1.54\times10^{-22}\ cm^3$), and $f(q)$ the normalized molecular form factor. In the usual small angle range, solvent molecules are too small to lead to a significant q-dependence ($f=1$), but in our case, DMAc molecules are bigger than, e.g. water molecules. To check this idea, we have plotted a master curve, i.e. the function $f(q)$ determined experimentally from each mixture. These curves are shown in the inset of Fig. 1, and can be seen to superimpose quite well. A Guinier fit of this function yields an average radius of gyration (R_g) of 2.4 Å, which corresponds to small spheres of radius (R) 3.1 Å (deduced from $R_g^2 = 3/5\ R^2$). This is not too far from the equivalent sphere radius of the solvent molecule calculated from v, 3.3 Å. The prefactor of $f(q)$ is found to be $0.7\ cm^{-1}$, slightly higher than the theoretically predicted value of $0.57\ cm^{-1}$ (Eq. (6)). Adding Eqs. (5) and (6) yields the fits also shown in Fig. 1, with satisfactory agreement. The reason why a characteristic size is observed for DMAc, and not for non-polar solvent of equivalent molecule size (e.g. toluene, etc…) can be a specific organisation of such polar organic solvent. To our knowledge, no similar observations for other solvents has been mentioned in the litterature.

3. Results and discussion

3.1. Synthesis of the polymer-grafted-SiO_2 nanoparticles

3.1.1. Nanoparticle functionalization

This two-steps reaction has been conducted in dimethylacetamide (DMAc), solvent in which the particles are dispersed (Scheme 1).

The first step consisted in the silanization of the particles with a thiol-containing silane. This is a relatively straightforward reaction, easy to control. We used a triethoxysilane because this is more efficient in terms of degree of grafting compared to a monoethoxysilane. Now, the drawback is the possibility to generate polycondensed silane network. Therefore, we investigated the structure of mercaptopropyl triethoxysilane (MPTS) layer onto the silica nanoparticles, depending on the degree of grafting, using ^{29}Si CP/MAS NMR.

From this NMR analysis, it appears that for the equivalent of 1 silane/nm^2, i.e. 6 wt% of MPTS, we get the formation of a monolayer, whereas when increasing this amount to 5 silanes/nm^{2,} i.e. 30 wt% of MPTS, polycondensed silanes layer is obtained. Details about the structural study of the grafted layer by ^{29}Si CP/MAS NMR has been given in a previous paper [33]. In conclusion, we ensured that grafting one silane per nm^2 or less (characterization of the layer with 0.5 silane per nm^2 has been done) led to the formation of a monolayer. Quantitative measurements of the grafting efficiency can be obtained from elemental analysis of sulfur and was found to be close to 100%.

The second step was an ‘over-grafting’ reaction which consisted in an esterification of the thiol group with the 2-bromoisobutyrate bromide. This reaction was shown to be more difficult. Running the esterification reaction cannot be done in the same conditions as usual when it has to be achieved in a colloidal suspension of silica nanoparticles in DMAc. Particularly, the addition of the basic catalyst was the critical point: most of the common bases, like triethylamine or pyridine, were found to be inefficient or to lead to the formation of a gel due to aggregation of the nanoparticles. The use of a more powerful base, dimethylaminopyridine (DMAP), gave more satisfactory results, especially when the reaction is conducted at 80 °C (grafting of the initiator moiety was 100% compared to the initial amount of thiol functions). It is reported in the literature that the better catalytic effect is not only due to the higher pK_a but also to the higher stability of the formed salts [34]. The reaction was conducted for 6 h and the purification was performed from ultra-filtration. By this method, we keep the particles in solution so that we avoid any drying of the particles that would lead to irreversible aggregation. Again,

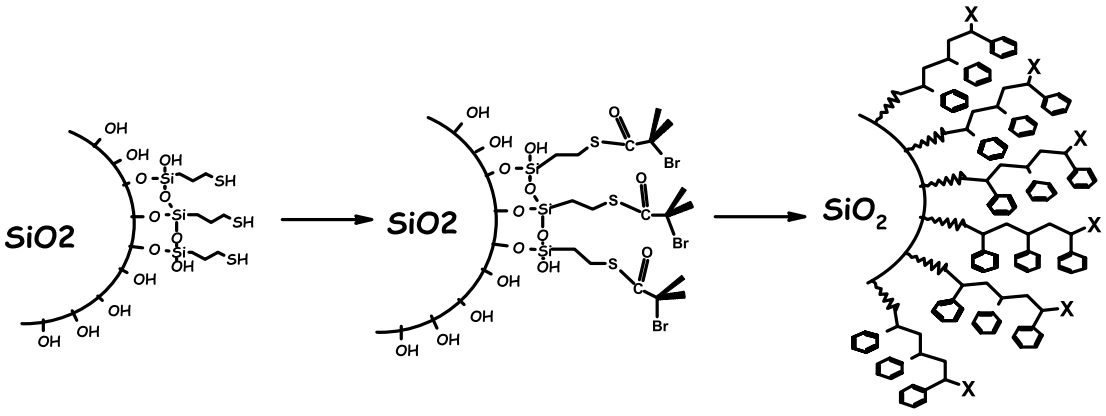

Scheme 1. Grafting of the initiator molecule via the 'over-grafting method'.

elemental analysis was used to determine the exact amount of grafted initiator (based on the amount of bromine).

We also performed infrared spectroscopy after the different steps of the initiator grafting (Fig. 2). The naked silica (spectrum A) shows different bands between 400 and 1700 cm^{-1}. The tetrahedron silica structure gives a signal of Si–O stretching (1116 cm^{-1}) with Si–O bending (472 cm^{-1}). We also observe the Si–OH bending at 966 cm^{-1} and the Si–O–Si bending at 800 cm^{-1}. The surface silanols groups give a broad band between 3000 and 3700 cm^{-1}. After addition of the mercapto-silane (spectrum B), we observed only absorption bands due to the C–H stretching (2850–2950 cm^{-1}). The presence of the thiol group could not be characterized from IR, as it absorbs preferentially in Raman. Nevertheless, spectrum C (over-grafting reaction) showed the presence of the carbonyl absorption band (1690 cm^{-1}).

3.1.2. 'Grafting from' polymerizations

We then conducted the polymerization of styrene and *n*-butyl methacrylate from the functionalized nanoparticles. Before doing this, we did some model polymerization in solution to optimize the ATRP of these monomers in these particular conditions (solvent, concentrations, initiator chemical structure). Results are not shown here but the best conditions (copper, ligand and initiator ratio) were found to be for the polymerization of styrene, 0.6:0.6:1 at 110 °C and for the polymerization of *n*-butyl methacrylate, 1:1:1 at 60 °C. In both cases, the semilogarithmic plot of monomer consumption with time is linear as well as the plot of number-averaged molecular weight (M_n) versus conversion where the M_n values were very close to the theoretical ones (note that for the *n*-butyl methacrylate, M_n values are slightly higher than the theoretical ones). Also, the molecular weight distribution remained very narrow through the polymerization process. We then verified that polymerization of styrene and *n*-butyl methacrylate in these conditions has the characteristics of a controlled/'living' polymerization.

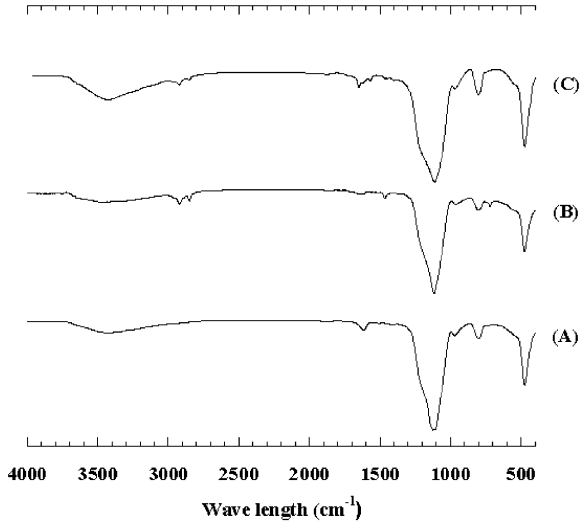

Fig. 2. FT-IR spectra of the naked silica nanoparticles (A), and the particles grafted from mercaptosilane (B), (2-bromo-thioisobutyryl) propane (C).

The polymerization from the functionalized silica nanoparticles has been done in the presence of free 'sacrificial initiator' because of the small concentration of grafted initiator and the necessity to generate enough copper II to induce the control of the polymerization.

The semilogarithmic plot of monomer conversion with time is linear during the whole polymerization process, attesting that a certain control has remained (Fig. 3). Table 1 reports the results obtained from polymerization of styrene from silica colloidal initiator. Grafted polymer chains (after removal of free chains by centrifugation) have been analyzed from GPC after etching with HF, following the procedure given by Patten [20]. It was found that molecular weights of the grafted chains were slightly higher than ones of the free chains. Generally (at least for the first four samples) molecular weight of both the grafted polymers and the free chains were higher than expected suggesting a low initiation efficiency. This is partly explained by the steric congestion and immobilization of initiators onto the surface of the particles. Not all of the initiator sites on the nanoparticle surface initiated the growth of polymer chains.

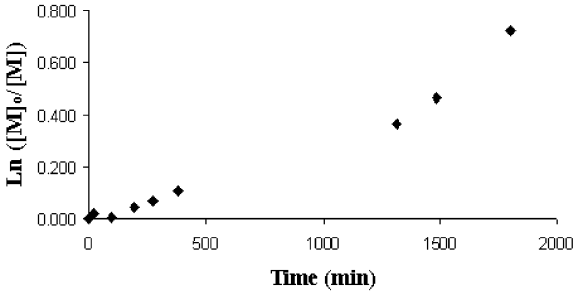

Fig. 3. Semi-logarithmic plot of monomer conversion versus time (stoichiometric ratios of 1670:1:1:1 for [styrene]:[I]:[Cu(I)]:[PMDETA]).

The growing chains sterically blocked the access of the catalyst to the neighboring initiation sites on the particle surface. Similar behaviour has been observed for the polymerization from silica nanoparticles [20,26]. Nevertheless, the polydispersity index (M_w/M_n) were also lower from the grafted chains, as compared to the one of the free chains.

Improvement of the control of the polymerization process has been done by changing the initial conditions, regarding the SANS experimental data. This is explained further in the text. The amount of polystyrene grafted onto the particles has been estimated from thermo-gravimetric analysis and was found to be 49.36% (sample 1 in Table 1). This corresponded to a total of 55 chains per nanoparticles.

3.2. Structural study via small-angle neutron scattering

3.2.1. SANS of functionalized beads

SANS characterization of the different reaction steps has been performed to attest of the colloidal stability. The first study has been done on silica particles with different degree of silanisation (3 and 30% w/w) compared to the naked one. Fig. 4 shows that the structure peaks are very closed and the

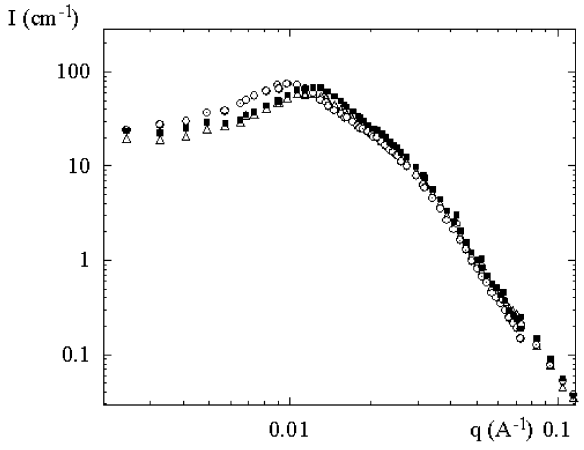

Fig. 4. Small angle neutrons scattering intensity from the silica dispersion at the different stages of the functionalization of the particles ($\Phi_{si}=2\%$) with mercaptopropyl triethoxysilanes (MPTS): (△) naked silica particles, (○) functionalized silica particles with 3% of MPTS, and (■) functionalized silica particles with 30% of MPTS.

form factor follows the same decrease (q^{-4}) in the three cases, which was expected given the small quantity of thiol-functional groups present at the interface (with respect to the mass of the silica beads) and given the poor contrast of such moieties with respect to the protonated solvent. With 3% of grafting, the maximum of the structure factor is shifted to the small wave-vectors values, while in the case of 30% of silane, the peak is shifted again toward the higher values of q. These minor changes in the low-q intensity speak in favor of a modification of the interparticle interactions, and maybe even some very limited aggregation (average aggregation number less than 2). Indeed the bare particles are stabilized through electrostatic repulsion. By grafting small molecules onto the surface, we replace this electrostatic repulsion by steric one. It seems that a certain amount of grafted molecules is necessary to get a similar effect (in terms of stabilization) by steric repulsion compared to the previous electrostatic one.

SANS has been carried out again after the 'over-grafting' step to verify the preservation of the colloidal stability, via the maximum of the interparticle structure factor. Results are detailed in a previous paper [33]. At high wave-vectors, both (grafted, over-grafted and bare particles) intensities superimposed rather well. Once the initiator was grafted (over-grafting), the intensity evolved somewhat towards higher intensity in the low-q range. This behaviour was compatible with a slight aggregation of two or three beads per aggregate (on average). We conclude that the solutions staid in the state of a well-controlled colloidal dispersion during these first two steps of the grafting.

3.2.2. SANS of the polymer-grafted-silica nanoparticles

3.2.2.1. Method. The scattering from structured nano-objects like polymer-grafted silica beads is non-trivial due to the number of contributions (beads, grafted polymer, free polymer, solvent mixtures), the interference between these, and the incoherent background generated by all of them. In order to decrease the amount of unknowns, we have started with a determination of the scattering length density ρ of the bare silica beads. Although the literature value of the density of macroscopic amorphous or crystalline silica is well-known, the importance of surface effects for small sizes and the possibility of density variations inside the bead may cause departures from macroscopic values for a given synthesis. Therefore, we have performed an external contrast variation (using H/D-solvent mixtures) at a fixed weight fraction of our silica beads. The incoherent background I_b was measured for each sample from the high-q limit, which is possible due to the quick decay of the coherent signal, proportional to q^{-4} in the Porod domain. Note that the shape of I_b was well described by Eqs. (5) and (6), with negligible variations with respect to the coherent signal. Then, the square root of the coherent intensity divided by the silica volume fraction was plotted against the solvent scattering length density. This plot of

Table 1
GPC data for the atom transfer radical polymerisation from silica nanoparticles in dimethylacetamide

Entry	Monomer	Conditions[a]	No. initiator/ nm^2	Moles eq initiator in sol.	Reaction time (h)	Conv. (%)[b]	$M_{n\ SEC}$[c]	M_w/M_n	$M_{n\ SEC}$ of cleaved chains [d]
1	Styrene	1670:1:1:1	0.15	6.67	30	50	10,6600	1.55	132,000 (1.28)
2	Styrene	1340:0.8:0.8:1	0.56	1.79	21	43.5	12,7000	1.51	144,100 (1.32)
3	Styrene	775:0.6:0.6:1	0.5	6	4	5.1	32,000	1.76	
4	Styrene	1460:0.6:0.6:1	0.5	3	4	8	48,600	1.61	66,000 (1.48)
5	Styrene	680:0.7:0.7:1	0.34	5.8	5	13.6	58,080	1.5	
6	Styrene	680:0.7:0.7:1	0.34	5.8	21	28	75,740	1.57	
7[e]	*n*-BuMA	388:0.7:1:1	0.34	2	7	19	11,200	1.15	

[a] Conditions correspond to molar ratios of monomer, 2-bromothioisobutyrate group on the silica colloid and in solution, Cu(I)Br, and PMDETA (ratios have been calculated from values given by elemental analysis).
[b] Conversion values are determined from gravimetric analysis.
[c] Molecular weight of polymer chains formed in solution.
[d] Molecular weight and molecular weight distribution in brackets, of grafted polymer chains after etching with HF.
[e] Sample 7 has been done using the conditions described in Section 3, i.e. the volume fraction of *n*-butyl methacrylate (*n*-BuMA) was 40%.

$\sqrt{([I(q_i)-I_b]/\Phi_{si})}$ is shown in Fig. 5 for different wave vectors q_i. The result is a group of linear fits crossing the *x*-axis at $\rho_{solvent}=\rho_{si}=3.4\times10^{10}$ cm^2, close to the literature value of 3.5×10^{10} cm^2. This experimental result was used for all other contrast calculations.

3.2.2.2. Results. SANS measurements allowed us to characterize the kinetics of the grafted polymerization procedure. Using contrast matching method described above, we could follow at the same time, structural change of silica beads and the grafted polymer. In this paper, we focused on the evolution of the scattering from the initial state before polymerisation is induced by heating to the final state of the polymerization.

A first series of SANS results deals with the aggregation state of silica beads. We therefore match the scattering length density of the solvent to the one of the polymer, using a mixture of hydrogenated and deuterated DMAc (53% h-DMAc/47% d-DMAc). Results are presented on Fig. 6 (a) for the initial state of polymerization and (b) for the final state of polymerization of non-deuterated polystyrene.

The absolute intensity I (cm^{-1}) has been divided by the product of the volume fraction of silica Φ_{sil} and by $\Delta\rho^2$. In both cases, $I/\Phi_{sil}\,\Delta\rho^2$ is very satisfactorily fitted, at large q, by an analytical expression of $\langle V_{sil}\rangle_w P(q)$, $\langle V_{sil}\rangle_w$ being the average volume and $P(q)$, the form factor of polydisperse silica spheres. The latter has been calculated and fitted to SANS measurement of bare silica particles [33]. In other words, for $q>1/R_{sil}$ a very similar shape to the one of native particles, is evidenced by the scattering. On the contrary, at low q the signal in Fig. 6(a) is larger than the calculation for individual particles; the slope is around 2. This indicates the presence of large aggregates with a fractal dimension close to what observed in a diffusion limited aggregation (DLA) process.

Compared to the initial state, the scattered intensity in Fig. 6(b) at low-q shows clearly a diminution of the intensity, i.e. of the aggregate size; this can be attributed to the effect of polymer grafting. Instead of a slope 2, the intensity presents a plateau at low q; extrapolation at $q\to0$ of $I/\Phi_{sil}\,\Delta\rho^2$ gives, in the absence of interactions between aggregates, the volume of aggregates, and thus a number of particles per aggregate of 3. In summary, grafting polymers on silica spheres has reduced aggregation and stabilized the colloidal dispersion.

A second series of measurements investigated the structure and conformation of the grafted polymer on particles. In this purpose, we used the possibility of matching the solvent to the silica beads. In this case, both deuterated and non-deuterated polystyrene are visible.

We showed in Fig. 7 the scattering curve at initial and final state of the grafting procedure for deuterated polymer (a) and non-deuterated polymer (b). From the initial state we observed a very flat signal, indicating an excellent match of silica beads. For the final state, we obtained a strong coherent signal, which is due to polymer chains, either grafted or in solution. Fig. 7(b) shows the same effects for non-deuterated polymer (silica is also matched): the initial

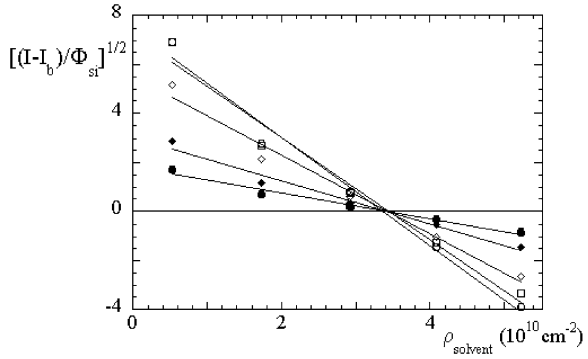

Fig. 5. Result of contrast variation experiment of NISSAN silica beads in different DMAc-H/DMAc-D mixtures. The square root of the coherent intensity per silica volume fraction $(I-I_b)/\Phi_{si}$ is plotted as a function of the solvent contrast. The zero of the family of straight lines yields the scattering length density of the silica.

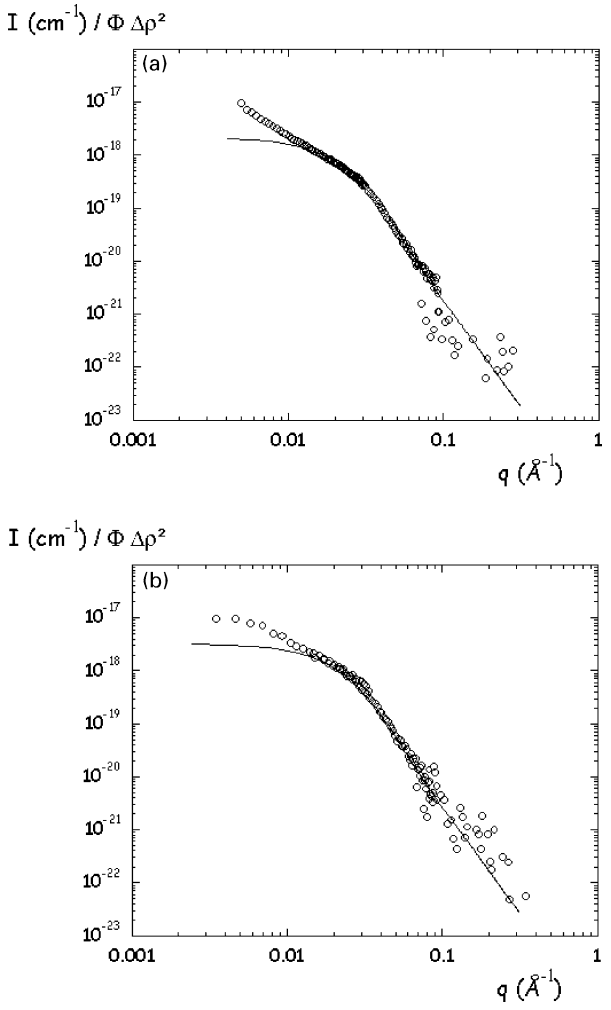

Fig. 6. Small angle neutron scattering intensity from the silica dispersion in polymer matching conditions (i.e. seeing the silica) at the initial step before polymerisation (a) and the final step of the polymerisation (b). Full line is the polydispersed form factor fit of the native silica $R=50.9$ Å and $\sigma=0.365$.

state shows flat scattering, the final one displays a shape close to the one of Fig. 7(a).

Fig. 8(a) represents in log–log plot, the same signal at the final stage of the polymerization using deuterated monomer (as in Fig. 7), and the signal from a deuterated polymer solution (volume fraction 3.2%). The signal of the polymer solution varies roughly as $q^{-1.65}$ at large q, which is consistent with theoretical value of $1/\nu=1.70$ where ν is the excluded volume exponent, and shows a plateau at low q. The crossover q value signals a characteristic size. Assuming that we were below overlapping concentration, the estimated value corresponds to a radius of gyration $R_g=30$ Å, which is correct regarding the molecular weight of the chains ($M_w\sim30{,}000$).

Compared to the polymer solution, the grafted silica scattering shows a strong scattering at low q (with a slope around 2.5). At high q, the contribution is analogous in slope to a polymer solution. At intermediate values, we can observe an additional strong shoulder (q around 0.02–0.03 Å^{-1}). This feature has some resemblance with the shoulder observed in the scattering from silica shown above. It may have several origins. We have first tried to fit the plot with a model of a polymer shell of thickness e wrapping a hollow sphere with the same average radius R_{sil} as silica beads. Compared to the genuine sphere, this object involves sizes $R_{sil}+e>R_{sil}$ which implies a shift of the position of the shoulder towards the low qs (larger sizes). Such a shift was not observed. A second origin could be that the density of the grafted polymer was not sufficient to observe a difference in scattering between the grafted chains and the free chains in solution. In this case, we could still have a signal from the holes in the polymer solutions, corresponding to the silica spheres. To decide between theses two hypotheses, it would be useful to subtract the signal of free chains in solution, estimated from the ratio of grafted initiators to free initiators (2:1). However, possible interactions between grafted chains and free chains and bead-polymer cross-correlation terms make a simple subtraction impossible. This illustrates the necessity to separate the free chains from the grafted particles in the sample before SANS measurements, e.g. by centrifugation.

The scattering in silica matching conditions with non-deuterated polymer (entry 5 in Table 1), and the corresponding free polystyrene (volume fraction 4.9%) is shown in Fig. 8(b). The pronounced shoulder at intermediate q, and the large q variation $q^{-1.65}$ are very similar to the one from deuterated chains (Fig. 8(a)). Again we could compare the fraction of grafted and free initiators (1 grafted initiator for 6 in solution) with the apparent fraction of polymer solution (85% of free chains). This fraction was completely different from the deuterated sample and made the signal closer to the scattering of polymer chains in solution.

In Fig. 8(a), the scattering in the low q regime is very strong with a large slope, of the order of 2.5 or even more. It indicates the presence of large fractal aggregates ($D_f=2.5$, see Eq. (3)). On the contrary, the low q scattering in Fig. 8 (b) is not important. We can remark that silica aggregates are small (3 particles) in this sample, as shown in Fig. 6(b).

As a summary, clearly some aggregation occurs at the beginning of the polymerization procedure (Fig. 6(a)). In Fig. 6(b), we see that aggregation decreased with polymerization conversion. Therefore, we could not avoid aggregation even after the functionalization procedure. We therefore conclude on the necessity to improve the synthetic procedure for a better control of the silica bead dispersion.

3.3. Improvements of the grafting procedure

In a second step, we have carefully adapted the synthetic conditions to avoid aggregation during the functionalization of the initiator. First, we have performed a series of tests to verify whether the colloidal suspension would be perturbed by the addition of the polymerization reactants (monomer, copper, etc…). We observed that the addition of copper without ligand

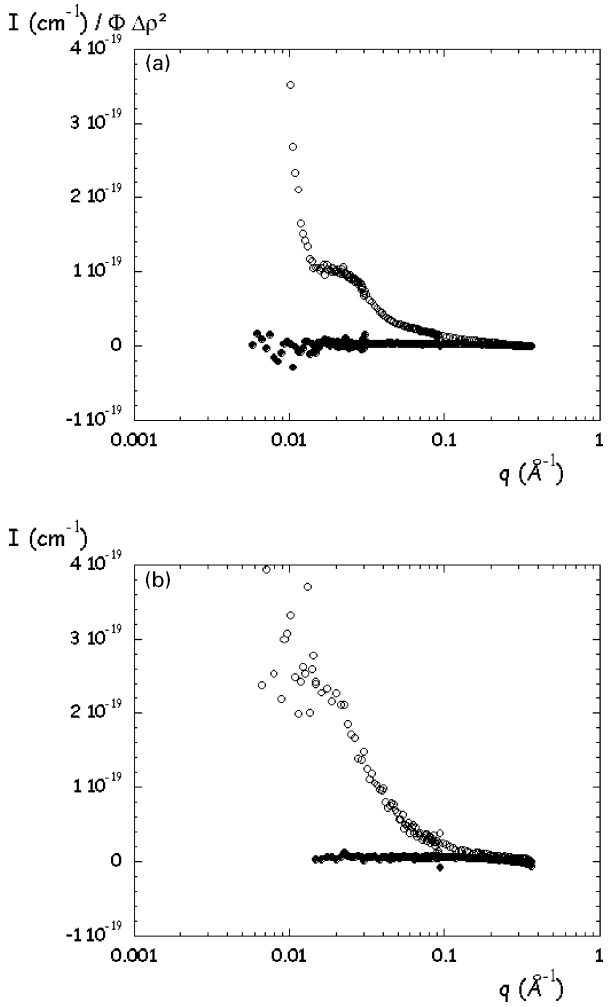

Fig. 7. Scattered intensity from the silica dispersion in silica matching conditions (i.e. seeing the polymer only) at the initial state before polymerisation (full circles) and at the final state of the polymerisation (open circles). Curve (a) is for a polymerisation procedure using deuterated monomer and (b) the same using non-deuterated monomer.

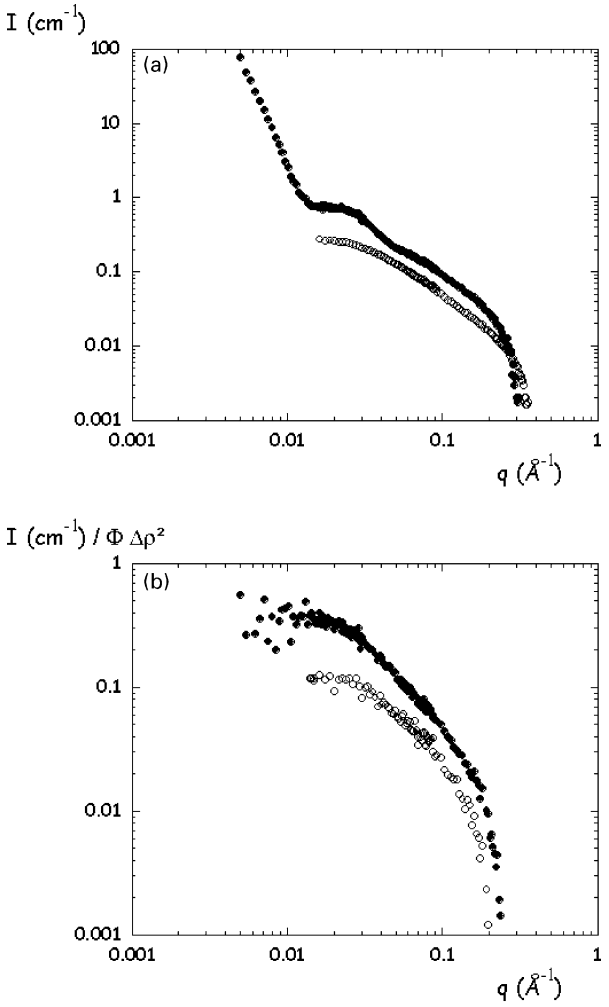

Fig. 8. Small angle neutron scattering from the silica dispersion in silica matching conditions at the final state of the polymerisation procedure (full circles) and scattered intensity by the polymer in solution in the same matching conditions (open circles). (a) is related to the deuterated polymer and (b) to the non-deuterated polymer. For the deuterated case, the signal of polymer in solution is shifted of a factor 1/3 which corresponds to the free chains volume fraction calculated from initiator ratios (see text for more explanations).

generally lead to gelation of the reaction. We interpret this as due to the strong affinity of copper (such as other metals) with thiols. These could be residual thiol groups that did not react during the esterification reaction. It is thus important to ensure that the copper is correctly liganted before adding the suspension of functional particles. This could be done by using a small excess of ligand, letting copper react with ligand in a small amount of solvent. The second critical point was the amount of monomer added to the solution. Indeed, the addition of styrene (or *n*-butyl methacrylate) would modify the polarity of the solution and generate flocculation of the particles. The addition was done slowly (dropwise) until the solution became cloudy. This occurred at 30% for styrene and 40% for *n*-butyl methacrylate (the difference is probably due to the higher polarity of the latter). Above this limit, phase separation occurred. Therefore, we carried out polymerization using these new conditions (entry 7 in Table 1). It was found that the polymerization was quantitative (the initiation step was efficient) and well controlled ($M_w/M_n = 1.15$). The solution remained transparent during the whole polymerization process and SANS measurements of that new sample are currently performed.

4. Conclusions

We have described a new route for preparing ATRP initiator-grafted-nanoparticles. In this work, we showed that every step of surface modifications and polymerization could be done with keeping the silica nanoparticles in solution. This was the best way to keep them well-dispersed and to limit the aggregation at a very moderate level. The dispersion of particles was checked using small-angle neutrons scattering at every stage of the functionalization.

SANS measurements made on the polymer-grafted particles has led to an understanding of the system behaviour during the polymerization procedure. These observations have permitted us to improve the synthetic conditions to get a better dispersion of the particles and a better control of the polymerization process. The SANS technique is well suited for the size range of interest here, and due to the unique possibility of contrast variation by H/D substitution we are able to highlight independently the contributions of the polymer layer and of the silica beads or aggregates.

Acknowledgements

We thanks France Costa-Torro (LCM, Université Pierre et Marie Curie) for the thermogravimetric analysis, as well as Ivan Klur and Armelle Pourpoint for Solid state ^{29}Si CP/MAS NMR (Rhodia, Centre de Recherche d'Aubervilliers). We are grateful to D. Clemens for the support during the SANS experiments at BENSC (HMI, Berlin). Support of this work by Région Ile de France, CEA and Rhodia is greatly acknowledged.

References

[1] Niemeyer CM. Angew Chem Int Ed 2001;40:4128.
[2] Mark JE, Lee C, editors. Hybrid inorganic-organic composites, vol. 585. Washington, DC: American Chemical Society; 1995.
[3] Kickelbick G, Schubert U. In: Baraton MI, editor. Synthesis, functionalization, and surface treatment of nanoparticles, vol. 1. Stevenson Ranch, CA: American Scientific Publishers; 2002.
[4] Schmidt G, Malwitz MM. Curr Opin Colloid Interface Sci 2003;8: 103.
[5] Edwards DCJ. Mater Sci 1990;25:4175.
[6] Voet A. J Polym Sci: Macromol Rev 1980;15:327.
[7] Auroy P, Auvray L, Leger L. J Colloid Interface Sci 1992;150:187.
[8] Prucker O, Ruhe J. Macromolecules 1998;31:602–13.
[9] Prucker O, Ruhe J. Macromolecules 1998;31:592–601.
[10] Ejaz M, Shinpei Y, Kohji O, Tsujii Y, Fukuda T. Macromolecules 1998;31:5934.
[11] Huang X, Wirth MJ. Macromolecules 1999;5:1694–6.
[12] Husseman M, Malmström E, McNamara M, Mate M, Mecerreyes D, Benoit D, Hedrick J, Mansky P, Huang E, Russell T, Hawker C. Macromolecules 1999;32:1424.
[13] Matyjaszewski K, Miller PJ, Shukla N, Immaraporn B, Gelman A, Luokala B, Siclovan T, Kickelbick G, Vallant T, Hoffmann H, Pakula T. Macromolecules 1999;32:8716.
[14] Zhao B, Brittain WJ. Prog Polym Sci 2000;25:677–710.
[15] Kong X, Kawai T, Abe J, Iyoda T. Macromolecules 2001;34: 1837–44.
[16] Mori H, Böker A, Krausch G, Müller AHE. Macromolecules 2001;34: 6871.
[17] Xiao D, Wirth MJ. Macromolecules 2002;35:2919–25.
[18] Carlmark A, Malmström E. J Am Chem Soc 2002;124:900–1.
[19] Kim JB, Huang W, Bruening ML, Baker GL. Macromolecules 2002; 35:5410–6.
[20] Von Werne T, Patten TE. J Am Chem Soc 2001;123:7497–505.
[21] Zheng G, Stöver HDH. Macromolecules 2002;35:6828–34.
[22] Vestal CR, Zhang J. J Am Chem Soc 2002;124:14312.
[23] Mori H, Chan Seng D, Zhang M, Müller AHE. Langmuir 2002;18:3682.
[24] Gu B, Sen A. Macromolecules 2002;35:8913.
[25] Ohno K, Koh K, Tsujii Y, Fukuda T. Macromolecules 2002;35:8989.
[26] Pyun J, Jia S, Kowalewski T, Patterson GD, Matyjaszewski K. Macromolecules 2003;36:5094–104.
[27] Percy MJ, Michailidou V, Armes SP, Perruchot C, Watts JF, Greaves SJ. Langmuir 2003;19:2072.
[28] Mori H, Müller AHE, Klee JE. J Am Chem Soc 2003;125:3712.
[29] Lui T, Jia S, Kowalewski T, Matyjaszewski K. Langmuir 2003;19: 6342.
[30] Pedersen JS, Gerstenberg MC. Macromolecules 1996;29:1363–5.
[31] Guinier A, Fournet G, editors. Small angle scattering of X-rays. New York: Wiley; 1955.
[32] Cotton JP. J Phys IV 1999;9:21.
[33] El Harrak A, Carrot G, Oberdisse J, Eychenne-Baron C, Boué F. Macromolecules 2004;37:6376.
[34] Scriven EFV. Chem Soc Rev 1983;12:129.